CHAPTER 2

EXPERIMENTAL AND CHARACTERIZATION TECHNIQUES

This chapter describes the experimental techniques which have been employed for the fabrication and characterization of ZnO NSs in this thesis work. First, RF magnetron sputtering technique has been extensively discussed for the fabrication of ZnO NSs and then the characterization techniques such as X-ray diffraction, field emission scanning electron microscope equipped with energy dispersive X-ray spectrometer, micro-Raman scattering, photoluminescence spectroscopy and homemade gas sensing setup that have been utilized for the investigations of ZnO NSs are briefly presented along with their basic principle.

2.1 Experimental techniques

RF magnetron sputtering is employed for the fabrication of ZnO NSs on different substrates under various growth conditions. The fabrication of ZnO NSs is associated to the following processes. They are

1. Choice of substrate
2. Target Preparation
3. Growth of ZnO NSs by RF magnetron sputtering

2.1.1 Choice of substrate

In the present work, the commercially available silicon wafers with (111) orientation and tin doped indium oxide (ITO) thin films coated glass plates (VIN KAROLA INSTRUMENTS) are used as substrates. The silicon wafers and ITO thin films coated glass plates are cleaved into 1 x 1 cm^2 substrates. The silicon (111) substrates are thoroughly cleaned by using the standard Radio Corporation of America cleaning procedures. ITO thin films coated glass substrates are also cleaned by acetone and ethanol for 15 minutes each. The cleaned substrates are dried under the stream of nitrogen.

2.1.2 Target preparation

In the present work, a 50 mm pure ZnO target has been used for the fabrication of 1-D ZnO NSs. This target is prepared by using the following steps.

- Planetary ball milling
- Pelletizing
- Sintering

Planetary ball milling

A ball mill is a type of grinder that is a cylindrical device used to grind or mix the materials like ores, chemicals, ceramic raw materials and paints. Planetary ball mill is smaller than common ball mill and mainly used in laboratories for grinding materials down to very small sizes and homogeneous powder mixtures. A planetary ball mill consists of at least one grinding jar which is arranged eccentrically on a sun wheel. The direction of movement of the sun wheel is opposite to that of the grinding jars. The grinding balls in the grinding jars are subjected to superimposed rotational movements.

In the present work, 30 gm of pure ZnO powder is taken in the grinding jar (stainless steel) with 8 zirconium oxide balls (10 mm diameter) that have been subjected to rotation for 60 cycles (30 min for 1 cycle) on both clockwise and anti-clockwise directions. The speed of the grinding jar is kept constant at 300 RPM. The difference in speeds between the grinding balls and jar produces the high and very effective degree of size reduction of the planetary ball mill. A planetary ball mill (Torrey Hills technologies, USA) having 4 jars with the volume of 100 ml, maximum rotation speed of a jar (600 RPM) and maximum rotation speed of sun wheel (300 RPM) has been used to homogenize the commercially available ZnO powders (Alfa Aesar, 99.999%).

Pelletizing

A 30 tons semi-automatic pellet press (Kimaya Engineers, Thane, India) has been used to make a 50 mm ZnO pellet as a target for sputtering

experiments. 1 gm of polyvinyl alcohol is mixed with the 10 ml of water and the final solution is heated to 80 °C that has been used as a binder. A few drops of binder are added to the grained ZnO powder and mixed uniformly. The final powder is filled into a cylindrical dye with the diameter of 50 mm and then pressed using motorized pellet press with the pressure of 15 tons for 300 sec.

Sintering

To harden the pressed pellet, it is sintered using two zone furnace at the temperature of 900 ºC for 6 hrs. The sintering temperature and time was optimized by the trial and error method. In order to evaporate the binder completely, the temperature of 230 °C has been maintained constant for 15 min. Then, the temperature was raised to 900 °C at a rate of 10 °C/min and maintained constantly for 6 hrs. At the end, the furnace is cooled down to room temperature naturally.

2.1.3 Growth of ZnO NSs by RF magnetron sputtering

2.1.3.1 Sputtering

Sputtering is a process which knocks out the surface atoms from the target material by bombarding it with ions having high kinetic energy. The sputtering process is illustrated in Fig. 2.1. The high energy kinetic ions are produced within the sputtering chamber by supplying the negative potential to the target material. Consequently, an inert gas within the chamber is ionized and the plasma is created. The positively charged ions within the chamber are accelerated towards the target material due to the negative potential. Subsequently, the collisions will occur between the positive ions and the target material and the energy is exchanged between them due to the inelastic collisions. The energy transferred to the target atom from the incident positive ions by the inelastic collision is given in the equation,

$$E_{transfer} = \frac{4M_i M_t}{(M_i + M_t)^2} \text{--------} (2.1)$$

where M_i and M_t are the masses of the incident ions and the target atoms respectively. If the energy transferred to the target atom or molecule by the incident ion is sufficient to overcome its surface binding energy, then the atom is sputtered out from the target material. The number of atoms sputtered from the surface of the target material per incident ion is called as sputtering yield [54].

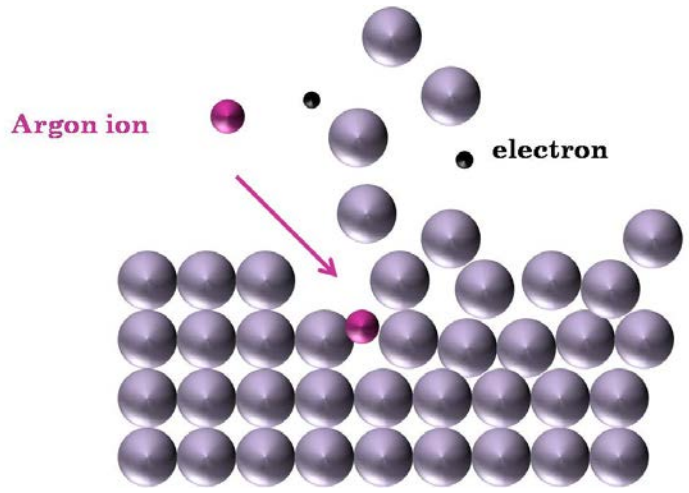

Fig. 2.1 Schematic representation of sputtering process

2.1.3.2 Magnetron sputtering

In the magnetron sputtering, the application of both electric and magnetic fields involve in addition to the conventional sputtering. The electric field can be either DC or RF as is required. The magnetic field is usually provided by arrangement of permanent magnets on the backside of the target material to enhance the sputtering efficiency by trapping the charge carriers from the plasma. The trapped electrons by the magnetic field lines follow cycloidal motion and increase the collision rate near to the target material with the sputtering gas molecules. Thus, the plasma density is increased and subsequently the sputtering rate is also increased. These trapped electrons can be sustained by the plasma at a lower pressure of 10^{-5} Torr. Further, the sputtered atoms from the surface of the target material are neutrally charged and hence they are unaffected by the magnetic trap. Furthermore, a significant amount of cathode power is lost

as heat in the conventional sputtering whereas in the magnetron sputtering, the cathode power is utilized much more efficiently. The overheating of the substrate due to the bombardment of secondary electrons is avoided by trapping the electrons near to the surface of the target material.

2.1.3.3 Types of sputtering

Magnetron sputtering can be classified into two types according to the potential applied to the target cathode.

- DC magnetron sputtering
- RF magnetron sputtering

DC magnetron sputtering

In the DC magnetron sputtering, as shown in Fig. 2.2, the target and substrate holder act as cathode and anode respectively. The ejection of atoms from the surface of the target material as a cathode by impinging of energetic positive ions of Ar gases under high DC voltage. The mechanism of this process involves a momentum transfer between the impinging energetic ions and the target materials that resulting the sputtering of surface atoms takes place.

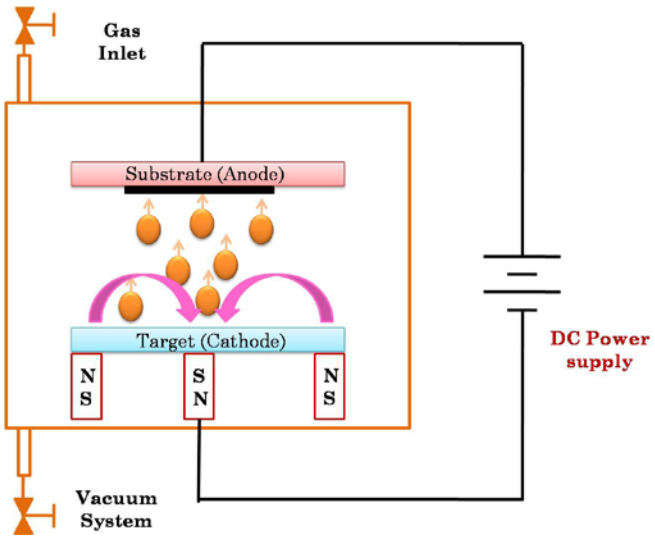

Fig. 2.2 Schematic diagram of DC magnetron sputtering

RF magnetron sputtering

In the RF magnetron sputtering, when an RF potential with a large peak to peak voltage is capacitively coupled to an electrode, an alternating positive and negative potentials appear on the surface of the cathode as well as target. During the part of each half cycle, the potential is such that ions are accelerated to the surface with enough energy to cause sputtering while on alternate half-cycles, electrons reach the surface to prevent any charge buildup. Commercially available 13.56 MHz radio frequency is often used for sputter deposition as shown in Fig. 2.3. RF sputtering can be performed at low gas pressures (<1 mTorr).

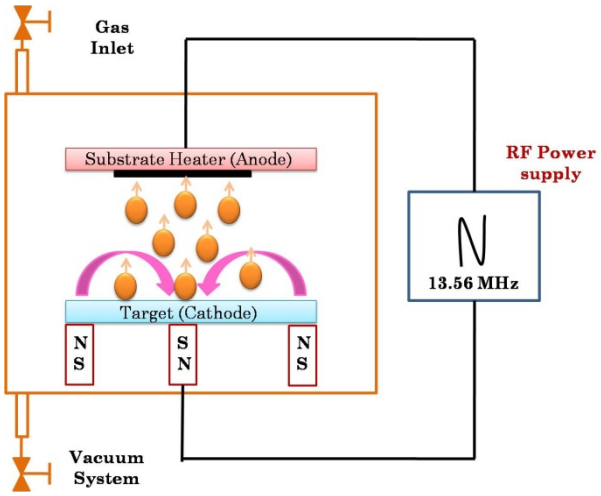

Fig. 2.3 Schematic diagram of RF magnetron sputtering

Advantages of RF magnetron sputtering

Magnetron sputtering can be done either in DC or RF modes. DC sputtering is done for conducting materials. If the target is a non-conducting material, then the positive charge will build up on the material and it will prevent sputtering. RF sputtering can be advantageous for both conducting and non-conducting materials. Here, magnets are used to increase the percentage of electrons that take part in ionization of events and thereby increase the

probability of electrons striking the inert gas which increase the length of the electron path and hence increase the ionization efficiency significantly.

Because of the several advantages, RF magnetron sputtering has been particularly employed to fabricate of ZnO NSs.

In this thesis work, a planar magnetron RF/DC sputtering unit (Hind High Vacuum Co. Pvt. Ltd., Bangalore, India) shown in Fig. 2.4 was used to deposit the ZnO NSs under various growth conditions. The important parts associated with the instrument are briefly discussed as follows [55].

Fig. 2.4 Photograph of a planar magnetron RF/DC sputtering unit

Rotary and diffusion pumps

HINDHIVAC direct driven, vane type rotary pump (Model ED 21 having a displacement capacity of 350 litres/min) is double state and oil sealed type. It can be employed to reach an ultimate vacuum of 10^{-3} mbar. During the operation, the rotor vanes sweep the volume of the gas or air trapped in the crescent shaped gap formed by the rotor which is mounted eccentrically in the

stator. As each vane passes the inlet port opening a known quantity of gas is introduced and subsequently trapped and compressed by the next vane following it and ejected via the exhaust flap valve mostly and via the interconnecting port to the II-stage partially, when the inlet pressure is near to atmosphere. As the inlet pressure drops the I-stage exhaust flap valve closes and all the air or gases pass to the II-stage, where it is further compressed and discharged to atmosphere.

HINDHIVAC oil diffusion pump (Model OD-150D having an effective pumping speed of 750 litres/sec with cryopump) is employed in the pressure range of 10^{-1} to 10^{-7} mbar. It consists of jet, boiler, heater, cold cap rings and thermostat. The oil in the boiler is heated by the heater and converted into vapor. This rises in the concentric columns and is limited by the jets due to the comparative high pressure existing above the boiler in the jet system. The vapor is forced through jet aperture where it is deflected downwards by the jet deflectors while the tubular side jet discharges vapor into the backing system. The molecules issuing from the jet engulf gas molecules, diffuse vapor streams not being able to diffuse back due to the downwards deflected vapors. The gas molecules are finally removed to the atmosphere by the rotary pump. The oil vapor impinging on the water cooled pump wall condenses and drained to the boiler where it is re-evaporated.

Pirani and Penning gauges

Pirani and penning gauges are employed for the measurement of low and high vacuum respectively. The HINDHIVAC mini pirani stabilized gauge model A6 STM is a pressure controlled instrument which is designed with the thermal conductivity type gauge head. This provides all necessary bridge circuits and signal conditioned analog outputs. This instrument works on the principle of change in resistance of material with a change in temperature. This can be used

to measure the vacuum from 0.5 to 0.001 mbar with suitable adopter. The HINDHIVAC mini penning stabilized gauge model STP4M-D is also a pressure controlled instrument which is designed with the cold cathode type gauge head. This gauge covers the vacuum range of $1x10^{-3}$ to $1x10^{-6}$ mbar in two ranges with instant range changing provided by a toggle switch.

Substrate heater

A specially designed 800 °C substrate heater cum holder of 2 in. diameter is attached with L-arm to move the substrate holder from magnetron source-1 to magnetron source-2 for multilayer deposition. It is resistively heated by the nichrome heating coil. It is kept inside the vacuum chamber and is located just above the line of eye-sight of magnetron. The distance between the substrate holder and magnetron can be adjusted. The heater has the capability of operating on 35 to 38 V AC with 6 amps maximum current through a step down transformer. The power terminals are taken out from the chamber via vacuum feedthrough. The power to the heater is controlled through solid state relay (SSR) and proportional-integral-derivative (PID) controller. The heater has a radiation shield which prevents heat loss in sideways and also helps to increase the uniformity of the heated surface. Samples are mounted by clips on the top surface of the heater which is made up of inconel 600 plate. K type thermocouple is placed behind the heating element at the same distance as that of the sample plate for consistent measurement of the sample temperature that is connected to the PID controller to monitor and control the substrate temperature.

Magnetron

HMAG-2000 is a 2 in. diameter magnetron source which can be operated both with RF power supply (RFG-500) and DC power supply (PS-2000). It is located inside the D type stainless steel chamber above which the target has to be placed. The magnetic field produced by this magnetron will be perpendicular to

the electric field produced by the RF/DC power supply. Hence, the electrons are trapped near to the magnetron and travels in a helical path as in cyclotron. Therefore, the ionization of Ar atoms near to the magnetron is increased that subsequently increases the plasma density and deposition rate as well as sputtering yield.

Magnetron power supply

Magnetron power supply [RF power supply (RFG-500) and DC power supply (PS-2000)] is designed to drive necessary power to magnetron source will all necessary interlocks and safety devices. The main advantage of HINDHIVAC planar magnetron sputtering unit is that the drastic reduction of secondary electrons is achieved by using proper shield. Hence, the substrates with low melting point can be used for the deposition of various materials since the heating of the substrates by the impingement of secondary electrons is avoided. Further, the magnetron power supply drives tight regulation superior arc quenching and low output energy. This helps vacuum coater to produce good thin, homogeneous, uniform, pure films of various materials. RF generator (Model HINDHIVAC RFG-500) is solid state protected against reflected power and highly reliable for continuous operation. Output of the RF generator is terminated matching to 50 ohms impedance. The output power of the RF generator can be varied from 0-500 Watts using the potentiometer. If there is a mismatch, then it will be shown in the reflected power meter. The reflected power can be reduced by adjusting the matching network.

Manual impedance matching network

The impedance of the chamber depends on the chamber dimension, nature of plasma and other various parameters. The output impedance of the RF generator is 50 ohms which should match with the input impedance of the load to create plasma. Hence, the impedance matching network is necessary for the

above purpose. HINHIVAC RF matching network is a manually adjustable LC network. A built in through the power meter indicates forward and reflected components and permits quick setting of various controls for optimum performance. By adjusting two capacitors of matching network alternatively reflected power can be minimized and forward power can be maximized.

Digital thickness meter

Digital thickness monitor (Model: DTM-101) allows improved manual control of the vacuum film deposition process by providing a direct display of deposition rate and film thickness during deposition. Semi-automatic control of film thickness can be accomplished by utilization of the shutter control relay in the monitor. The shutter control relay allows for direct operator control of the system shutter and will also automatically close the shutter when the deposition thickness equals a pre-programmed value. The DTM-101 has two shutter control relays which can be programmed to close on two separate set points. The monitor requires some operator supplied parameters such as tooling factor, density and acoustic impedance of the depositing material in order to direct read out and shutter control. Entry, modification and display of these parameters are easy and straight forward. Parameters storage is not dependent on continuous AC power since it has an internal, self charging, Ni-Cd batteries which provide parameter storage for a minimum of 60 days without external power.

For the fabrication of vertically aligned ZnO NSs by RF magnetron sputtering technique, the deposition pressure and substrate temperature are varied. The growth parameters used for the fabrication of NSs are listed in the following Table 2.1. The detailed growth conditions for the fabrication of 1-D ZnO NSs are described in the corresponding chapters.

Table 2.1 Deposition parameters of RF magnetron sputtering for the fabrication of ZnO NSs.

Description about the deposition conditions	
Sputtering Target	2 in. pure ZnO (99.999%)
Base pressure	5 x 10^{-6} mbar
Deposition pressure	0.001-0.1 mbar
Substrate – Target distance	50 mm
Substrate temperature	Room temperature to 650 °C
RF power	60 - 150 Watts
Sputtering gas	Argon
Reactive gas	Oxygen
Growth duration	60 min

2.2 Characterization techniques

2.2.1 X-ray diffraction (XRD)

XRD is a primary and powerful tool to investigate the crystalline structure of the materials. It is mainly used to determine the crystalline quality, phase orientation, lattice parameters, strain and composition of alloys [56]. X-rays are electromagnetic radiation that has a wavelength range of 0.01 to 10 nm. X-rays are typically used to the lattice diffraction due to its wavelength very close to the atomic spacing. The scattered X-rays from the crystal lattice planes will form the constructive interference patterns by fulfilling the Bragg's law as shown in Fig. 2.5.

$$2d\sin\theta = n\lambda \text{ ----------(2.2)}$$

X-rays are generated in a cathode ray tube by heating a filament to produce electrons which is accelerated towards the target material such as Cu, Fe, Mo, and Cr by applying a voltage and bombarded with the target. When electrons have sufficient energy to dislodge inner shell electrons of the target material, the characteristic X-ray spectra are produced. The specific wavelengths are the characteristics of the target material.

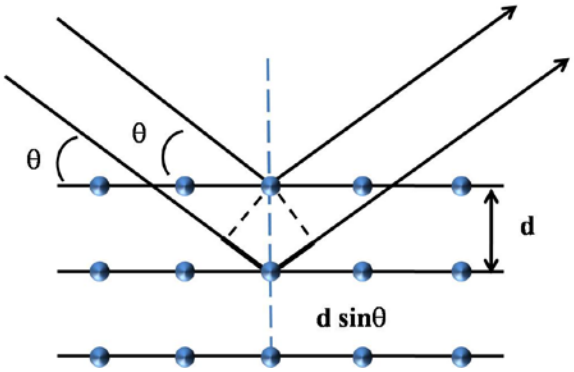

Fig. 2.5 Schematic diagram for determining Bragg's law

To produce coherent and monochromatic X-rays, the generated X-rays are filtered by the crystal monochromator. Copper is the most common target material for single crystal diffraction with Cu K_α radiation = 1.5406 Å. These X-rays are collimated and directed onto the sample. As the sample and detector are rotated, the intensity of the reflected X-rays is recorded. When the geometry of the incident X-rays impinging the sample satisfies the Bragg's equation (2.2), the constructive interference occurs which provides the signal to a detector. A detector records and processes this X-ray signal and converts the signal to a count rate which is then given as output to a device such as a printer or computer monitor.

Here, the crystalline nature and phase orientation of the NSs are analyzed by a Rigaku X-ray diffractometer with Cu K_α radiation of wavelength λ=1.5406 Å. The diffraction patterns are recorded using θ-2θ geometry between 10° and 80° with step size of 0.05° for the structural identification.

2.2.2 Scanning electron microscope (SEM)

SEM enables the investigation of specimens that uses electrons to produce clear and less electro-statically distorted images with high spatial resolution down to 1 nm. The path ways of the electron beams are controlled using electromagnetic lenses. The electrons are generated using a filament and

are accelerated by the anode potential. The accelerated electron beams are then focused by electromagnetic lenses capable of bending the electron beams, as is illustrated schematically in Fig 2.6 [57]. Ultra high vacuum is essential for the electrons to progress along the column without any perturbations and prevents discharging within the chamber. In the SEM, the electron beam is focused to a fine point and swept across the specimen in a raster scanning procedure.

When these narrower beams of primary electrons impinge on the specimen, it undergoes both the elastic and inelastic collisions with the specimen. The energy exchange between the electrons and the specimen resulting in different mechanisms including reflection of high energy electrons, emission of secondary electrons, back scattered electrons, Auger electrons and X-rays, each of which can be well detectable by appropriate detectors. However, the secondary electrons, due to the inelastic interaction between electrons and the specimen, with an energy of (<50 eV) are usually emitted from the k-shell of the specimen atoms and its features such as angle and velocity are related to the surface features of the specimen. A detector detects the secondary electrons and produces an electronic signal. This signal is further amplified and transformed to a video-image that can be seen as images on the monitor. The resolution of the SEM image is dependent on the probe size of the beam which depends on the wavelength of the electron and the lens and aberrations in the electro-optic system that produces the electron beam. Further, the material should necessarily be conductive since the incident electron beam induces the charging effects for the non-conducting materials. In this thesis work, Carl Zeiss-Σigma model equipped with LaB_6 field emission gun was used to examine the surface morphology of the NSs.

2.2.3 Energy dispersive X-ray spectroscopy (EDX)

As the electron beam of the field emission source impinges on the specimen, it ejects an electron from the K- or L- shell of the atoms and leaves a

vacancy on that shell. Subsequently, an outer shell electron jumps to compensate the vacancy which is created on the atomic orbitals that emits the X-rays. The each X-ray photon is characteristic of the element that produced it. The EDX microanalysis system collects X-ray photons, classifies and plots them by energy. The energies of the characteristic X-rays allow the elements making up the sample to be identified, while the intensities of the characteristic X-ray peaks allow the concentrations of the elements to be quantified.

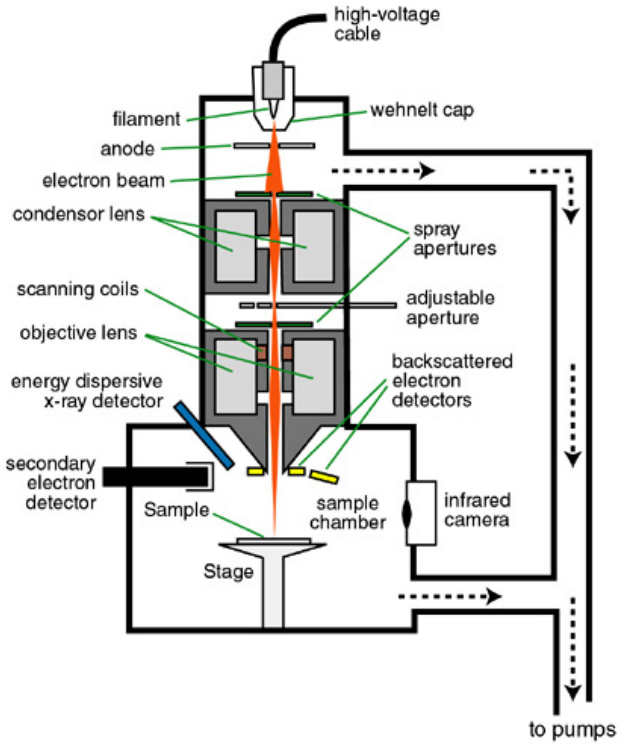

Fig. 2.6 Schematic diagram of SEM

Here, EDX spectrum was recorded with the accelerating voltage and the working distance of 10 keV and 8 mm respectively for the easy detection of signal by the silicon drift detector (SDD) which has high resistivity silicon chip where electrons are driven to a small collecting anode. The advantage lies in the extremely low capacitance of this anode, thereby utilizing shorter processing times and allowing very high throughput. The detector (Oxford Instruments-10

mm^2 SDD detector - x-act) engaged in this measurement is cooled by thermoelectrically that is free from liquid nitrogen.

2.2.4 Micro-Raman scattering

Raman spectroscopy is a non-destructive and powerful technique to analyze the optical and crystalline qualities of the materials from their unique vibrational and rotational energy level structure. This Phenomenon is discovered by the Indian physicist sir C. V. Raman in 1928.

Raman scattering utilizes the inelastic scattering of monochromatic electromagnetic waves. When the monochromatic light interacts with the sample, the phonons in the samples introduce a shift in the energy of the photon. This energy shift represents the information about the vibrational modes in the sample. The intensity of the inelastically scattered light is weak and is represented as a function of the frequency shift.

Room temperature micro-Raman spectrum was recorded using a LabRam HR 800 micro-Raman spectrometer in the back scattering geometry within the spectral range of 75 - 700 cm^{-1}. He-Ne laser (λ = 632.8 nm) with a power of 17 mW was used as an excitation source and the laser beam was focused through a microscope (100X) with a spot size of ~1 μm. The inelastically scattered signal is dispersed by a 1800 lines/mm grating in a monochromator (HORIBA JOBIN YVON). This dispersed signal is detected by the thermoelectrically cooled charge coupled device (CCD) detector.

2.2.5 Photoluminescence spectroscopy

Photoluminescence (PL) spectroscopy is a contact-less, non-destructive method to probe the optical properties of the semiconducting materials. When the photons from the monochromatic light source incident on the semiconducting materials and excite the electrons to the allowed excited states. This process is called as photo-excitation. The photo-excitation process creates

the electron-hole pairs in the semiconducting materials and these electrons and holes are accumulated on the conduction band minimum and valence band maximum respectively. These excited electrons from the conduction band minimum return to its equilibrium states by releasing the excess energy in the form of light or luminescence which may be radiative or non-radiative process. This luminescence is called as PL. The energy of the emitted light is related to the difference in energy levels of excited and equilibrium states. This is a powerful technique to determine the band gap, exciton recombination mechanism and defect levels [58].

Fig. 2.7 Photograph of the photoluminescence spectrometer

Fig. 2.7 shows the photograph of a PL spectrometer assembled in our laboratory. A 325 nm wavelength He-Cd laser (Kimmon Koha Co., Ltd., Japan) with an output power of 30 mW is used as an excitation source. The additional plasma lines from the excitation source are filtered by a 325 nm interference filter. After this, the laser light is focused on the samples by the condenser lens. The samples are kept in an optical cryostat (Janis Research Company Inc., USA) which can be cooled down to low temperatures up to 10 K. In order to avoid the direct impingement of the reflected laser beam from the sample into the perpendicularly arranged monochromator, the optical cryostat is positioned at

slightly greater than 45° to the incoming laser light. The luminescence signal from the samples is passed through the edge filter with the cut-off wavelength of 325 nm in order to filter the wavelength below the laser light and dispersed by a 1200 lines/mm grating in a 0.55 m monochromator (HORIBA JOBIN YVON). This dispersed signal is detected by the thermoelectrically cooled charge coupled device.

2.2.6 Physical Property Measurement System (PPMS) – Vibrating Sample Magnetometer (VSM)

PPMS (Quantum Design, USA) stands for an unique concept in measuring various physical properties such as magnetic and transport properties with the specially designed measurement options. Sample background includes fields up to ± 90 kOe and temperature range of 1.9 – 400 K. Its advanced flexible design combines many features in one instrument that makes the PPMS as most versatile system. The PPMS has following features that are the sample chamber with 2.6 cm diameter sample access, pulse tube (PT410, Cryomech, UK) cryogen-free cooling technology and versatile sample mounts coupled with 12 electrical leads build into the chamber insert. The Model 6000, a microprocessor-controlled device contains current or voltage sources that control the PPMS with an integrated Visual basic interface with the Windows based MultiVu software.

The VSM P525 (Quantum Design, USA) option for the PPMS measurements of the sample primarily consists of a linear motor transport (head) for vibrating the sample, a coil set puck for detection, electronics for driving the linear motor transport and detecting the response from the pickup coils, and a copy of the MultiVu software application for automation and control.

The VSM measurement is achieved by oscillating the sample near to the pickup coil and the induced voltage is detected synchronously. The compact pickup coil configuration has relatively large oscillation amplitude (1-3 mm

peak) and frequency of 40 Hz, the system is able to resolve the magnetization changes of less than 10^{-6} emu at a rate of 1 Hz.

Principle of VSM and Measurement procedure

The basic principle of a VSM is the Faraday's law of induction [59,60] which is described as

$$V_{coil} = \frac{d\phi}{dt}$$

where V_{coil} and ($d\phi/dt$) are the induced voltage and change in magnetic flux respectively.

The sample is placed in the middle of the paddle shaped sample holder. The sample holder is placed inside a uniform magnetic field to magnetize the sample. The magnetization of a sample increases with increasing magnitude of the field and the change in magnetic flux induces a voltage signal which is measured by the pickup coil located near to the sample. The signal is usually weak and is amplified by the lock-in amplifier at a particular frequency. The signal measured by the pickup coil is directly proportional to the magnetization of the sample and is independent to the applied external magnetic field.

The magnetic property measurements of the samples are carried out both in zero field cooled (ZFC) and field cooled modes. In ZFC mode, the sample is initially cooled in zero magnetic field to 2 K and then the data is recorded while warming in the presence of external magnetic field whereas in the case of FC mode, the data is recorded upon cooling without removing the applied external magnetic field. The temperature dependent magnetization curves of the samples are recorded at constant field strength of 1000 Oe. ZFC and FC magnetization curves are recorded at a constant temperature range of 2-300 K with the sweep rate of temperature is 1 K/min.

2.2.7 Resistance based gas sensor set-up

Fig. 2.8 shows a schematic diagram of the resistance based gas sensor set-up. It is constructed using Keithley's source meter (Model:2400), mass flow controllers (MKS, USA), test chamber and heater with temperature controller. In order to fabricate metal-semiconductor-metal resistance based gas sensor, In/Al (50/250nm) contact electrodes were deposited on top of the samples using the e-beam evaporation system via multi-finger mask to form inter-digital sensor, both electrodes finger and finger-to-finger gap was maintained at 30 μm as shown in Fig. 2.9.

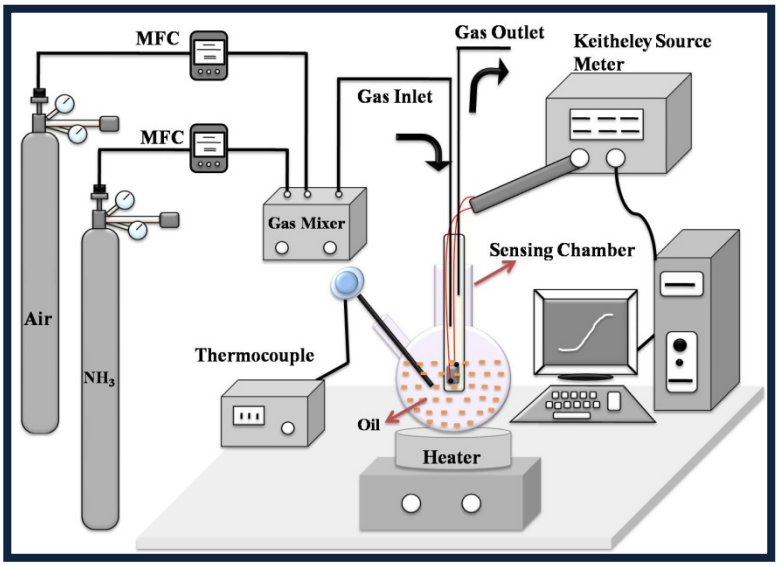

Fig. 2.8 Schematic diagram of the resistance based gas sensing set-up

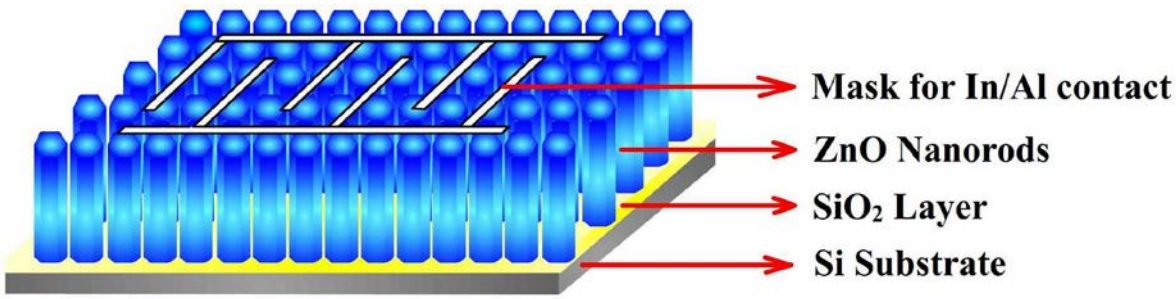

Fig. 2.9 Schematic diagram of the ZnO nanostructures based gas sensing device

The sensor studies were carried out under various concentrations of NH_3 gas and the air as the diluents at different temperatures ranging from room temperature to 150 °C. The flow rate of the gases inside the test chamber was controlled by the mass flow controllers (MKS, USA). The resistance of the gas sensors was determined by measuring the electric current with respect to gas ambient for the sweep potential difference from -10 to 10 V. The sensitivity was calculated by the following standard equation.

$$\text{Sensitivity (\%)} = \left(\frac{\left(R_{gas} - R_{air}\right)}{R_{air}} \right) X100 \text{----------(2.2)}$$

The response and recovery times of a sensor were defined as the time taken for reaching the sensors output to 90% of the equilibrium value after injecting and removing the testing gas respectively.

2.2.8 Photocatalytic experiment

The photocatalytic activity, efficiency and photostability of the vertically aligned ZnO NRs grown on silicon substrates were investigated from the degradation of organic dyes such as methylene blue (MB), Rhodamine B (RhB) and methyl orange (MO) under various irradiation sources of light such as visible and solar light. Samples of degraded dye solutions were taken after different time intervals and their absorbance spectra were recorded by the UV-Vis spectrometer to evaluate their degradation rates.

4 ml of 5 mg/L dye solutions were taken in a two separate test tubes and 1 x 0.5 cm^2 size of substrate containing ZnO NRs (average diameter = 129 nm, average length = 680 nm and density = 2 x 10^9 NRs/cm^2) was immersed into the solution separately. The test tubes were placed at ~16 cm far away from the light source to cancel the heat. The irradiation of visible and sunlight was done with 300 W tungsten halogen lamp (8500 lumen) and natural bright sunlight (12.00 to 4.00 P.M.) respectively. The degradation of dye molecules was analyzed by recording UV-Vis absorption spectrum using Shimadzu UV-2450

spectrophotometer at the given interval of time. To examine the photocorrosion and photostability of the vertically aligned ZnO NRs as a potential catalyst, the photocatalytic degradation of MB was repeated for 10 cycles under the irradiation of visible light.

The absorbance of a solution is directly proportional to the concentration of the compound in the solution, as described by the Beer-Lambert Law:

$$A=\varepsilon bC \text{ ---------- } (2.3)$$

where *A* is absorbance (no units), ε is the molar absorptivity (L mol^{-1} cm^{-1}), *b* is the path length of the sample solution in the cuvette (cm), and *C* is the concentration of the compound in the solution (mol L-1).

The percentage of degradation and degradation rate can be calculated by the following equations [61].

$$\% \text{ of degradation} = \frac{C_0 - C}{C_0} X100 \text{ --------- } (2.4)$$

where C_o and C are the initial and final concentrations of the dye solution (mol L^{-1}) respectively.

2.3 Summary

The first part of the chapter is devoted to describe the experimental techniques involved for the fabrication of ZnO NSs by RF magnetron sputtering. The basic requirement for the growth of ZnO NSs by sputtering is a 2 in. ZnO sputtering target which is prepared via a simple solid state reaction technique using commercially available ZnO powder (ZnO, 99.999%) as a source materials. The argon and oxygen gases are used as sputtering and reactive gases for the fabrication of ZnO NSs. The commercially available n-type Si(111) and ITO coated glass plate are used as a substrate for the fabrication of 1-D NSs. The second part of this chapter describes the characterization techniques in which the important methods used for the analysis of ZnO NSs. The crystalline nature and phase orientation of the ZnO NSs are investigated by X-ray diffractometer with Cu K_α radiation of wavelength λ=1.5406 Å. Field emission scanning electron microscope (FESEM) equipped with energy dispersive X-ray spectrometer has been used for the morphological and elemental analysis of the NSs.The basic principle and instrumentation of the micro Raman scattering and temperature dependent photoluminescence (TDPL) have been discussed. Resistance based gas sensor setup has been constructed and utilized for the NH_3 gas sensing applications using ZnO NSs. In addition to the gas sensing properties of ZnO NSs, the experimental condition for the photocatalyst behaviour of ZnO NRs has been studied for various dye molecules under the irradiation of visible and sun light.